

# Morphology Control of One-Dimensional Peptide Nanostructures

Tae Hee Han, Ji Sun Park, Jun Kyun Oh, and Sang Ouk Kim\*

Department of Materials Science and Engineering, KAIST Institute for the Nanocentury,  
KAIST, Daejeon 305-701, Republic of Korea

Self-assembly of peptides has gathered particular attentions since it may provide unique properties relying on highly specific molecular recognition and structural organization. Peptides assemble into complex nanostructures through highly specific biomolecular interactions such as hydrogen bonding and hydrophobic interaction. Among various nanostructured materials, one-dimensional nanostructures, such as nanowires, nanotubes, and nanoribbons, have been intensively investigated. However, so far, systematic investigations on the morphological variation of peptide-assembly have rarely been explored. Here we demonstrate the morphological diversity of the self-assembly of an aromatic peptide unit. The aromatic dipeptides spontaneously assembled into nanotubes, nanoribbons, and nanowires in various polar solvents. Our work provides a broad spectrum of one-dimensional nanostructured materials, which are potentially significant for nanofabrication.

**Keywords:** Peptide Assembly, One-Dimensional Structures, Solvent Polarity.

## 1. INTRODUCTION

Self-assembly of biomolecular building blocks has attracted much attention since it may provide unique chemical and biological functionalities relying on highly specific molecular recognition and structural organization.<sup>1–3</sup> In particular, peptides have been reported to assemble into various well-defined nanostructures including nanofibers,<sup>4–6</sup> nanotubes,<sup>7–11</sup> closed-caged spheres,<sup>12,13</sup> and so on. Because of the easy modification of their chemical and biological functionalities, peptide nanostructures have been utilized for various applications including drug transporters,<sup>14</sup> scaffolds for tissue engineering,<sup>15,16</sup> sensing devices for biological molecules,<sup>17</sup> etc.<sup>18,19</sup> Moreover, unlike inorganic nanomaterials, which usually require severe synthetic conditions, peptide-assembly may generate a variety of functional nanostructures in an environmentally benign process. Aromatic dipeptide consisting of two successively connected phenylalanine units has been regarded as an important building block for nanofabrication.<sup>20</sup> The dipeptide was introduced as the  $\beta$ -amyloid structural motif associated with Alzheimer's disease. The aromatic dipeptides have been reported to form robust nanotubes in aqueous solution and can be applied as a useful template material for casting metallic nanowires. Recently, we have presented liquid crystalline

peptide nanowires prepared from the dipeptide unit.<sup>21</sup> Despite the potential significance of this peptide unit, however, the systematic investigation on the morphological evolution of the aromatic dipeptide has been rarely explored so far.

Here we demonstrate the synthesis of a variety of one-dimensional peptide nanostructures. Diverse morphologies were simply prepared by dissolving the aromatic dipeptide in various polar solvents. Our work provides a broad spectrum of nanostructured materials which are potentially significant for nanofabrication.

## 2. EXPERIMENTAL DETAILS

### 2.1. Materials

The lyophilized form of the NH<sub>2</sub>-Phe-Phe-COOH dipeptide was purchased from Bachem (Bubendorf, Switzerland). Methanol, ethanol, and dichloromethane (CH<sub>2</sub>Cl<sub>2</sub>) were purchased from Aldrich Chemical Co. and used as-received. Water was deionized by using Milipore MilliQ®.

### 2.2. Peptide Nanostructure Preparation and Characterizations

We dissolved aromatic dipeptide by sonicating for 20 min, subsequently stirring it with a magnetic bar at 60 °C until

\* Author to whom correspondence should be addressed.

the vial turned completely transparent. During the slow cooling of vial to room temperature, nanostructures were formed in the vial. Peptide nanostructures were prepared from a concentration of  $4 \text{ mg mL}^{-1}$  in  $\text{H}_2\text{O}$  and  $\text{CH}_2\text{Cl}_2$ , and  $10 \text{ mg mL}^{-1}$  in methanol and ethanol. The morphology of dipeptide nanostructures was analyzed by a field emission scanning electron microscopy (Hitachi S-4800, Japan). Carbon coating was performed to enhance scattering contrast and electric conductivity (CED 030 carbon evaporator, Bal-tec, Germany). FT-IR was accomplished with a JASCO FT-IR 470 Plus spectrometer at room temperature to investigate intermolecular interaction. Samples for FI-IR were prepared by mixing peptide nanostructure with KBr (Aldrich Chemical Co.) and subsequently pressing into a pallet. The difference in the crystal structure was shown with powder X-ray diffraction (XRD). The samples for powder XRD were prepared by evaporating the solvent of the peptide solution and subsequently grinding the residue. The X-ray diffraction measurements were performed on a Rigaku D maxIIIc powder diffractometer with  $\text{CuK}_\alpha$  radiation ( $\lambda = 1.5418 \text{ \AA}$ ).

### 3. RESULTS AND DISCUSSION

Figure 1 shows the SEM images of diverse one-dimensional nanostructures formed in different solvents. Figure 1(a) presents nanotubes, whose diameter ranges

from 100 nm to  $5 \mu\text{m}$ . Their length varies from hundreds of nanometers to one hundred microns. The inset of Figure 1(a) reveals that the nanostructure obtained in water has tubular structure. The nanoribbons formed in methanol are shown in Figure 1(b). The cross section of the thin nanoribbons showed a rectangular shape with width ranges from 100 to 1000 nm. Nanoribbons were mechanically flexible, which contrasts to the highly rigid nanotubes. Figure 1(c) shows nanoribbons obtained in ethanol. The inset of Figure 1(c) represents the cross sectional morphology of a flat nanoribbon. Figure 1(d) shows the mixed morphology of nanowires and nanoribbons prepared in  $\text{CH}_2\text{Cl}_2$ . Our results clearly demonstrate that the aromatic dipeptide assembled into different morphologies in various polar solvents.

The solvent parameters considered crucial for studying solvent–dipeptide interactions are summarized in Table I.  $E_T(30)$  based on the solvatochromic measurement of the pyridinium *N*-phenoxide betaine dye is the most comprehensive and widely used solvent scale to indicate the polarity of a solvent.<sup>22,23</sup> The normalized  $E_T^N$  scale is defined by extreme reference solvents water and tetramethyl silane (TMS) as follows:  $E_T^N = (E_T(30) - E_T(30)_{\text{TMS}})/(E_T(30)_{\text{water}} - E_T(30)_{\text{TMS}})$ .<sup>22,23</sup> Solvent acidity (SA scale)<sup>24</sup> and basicity (SB scale)<sup>25</sup> are related to the strength of hydrogen bonding.<sup>23,26</sup> Water and methanol are highly polar solvents, while  $\text{CH}_2\text{Cl}_2$  is much less polar. The solvent molecule of  $\text{CH}_2\text{Cl}_2$  has a low tendency to

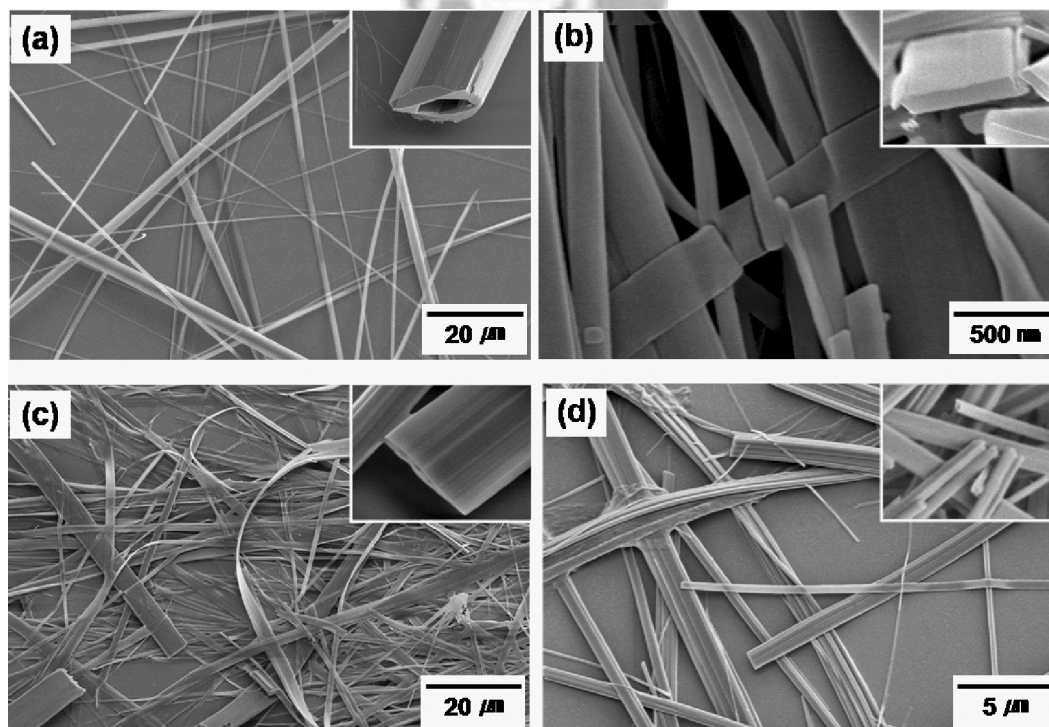


**Fig. 1.** Morphologies of diverse nanostructures formed in the various solvents: (a) Nanotubes (water), the inset image represents the hollow tubular structure. (b) Nanoribbons (methanol). (c) Nanoribbon (ethanol), the inset image shows the flat nanoribbon. (d) Nanoribbons and nanowires formed in  $\text{CH}_2\text{Cl}_2$ .

**Table I.** Solvent properties: The  $E_T(30)$  is the empirical parameter of solvent polarity [ $\text{kcal mol}^{-1}$ ] and  $E_T^N$  is the normalized parameter of solvent polarity. Solvent acidity (SA scale) and solvent basicity (SB scale) are related to the strength of hydrogen bonding.

	$E_T(30)$	$E_T^N$	SB	SA
$\text{CH}_2\text{Cl}_2$	40.7	0.309	0.178	0.040
EtOH	51.9	0.654	0.658	0.400
MeOH	55.4	0.762	0.545	0.605
Water	63.1	1	0.025	1.062

form a hydrogen bond with an aromatic dipeptide as indicated by the lowest value of SA and SB. Nanotubes were fabricated in highly polar water [ $E_T(30) = 80.0$ ]. Nanoribbons were prepared from methanol [ $E_T(30) = 55.4$ ] and ethanol [ $E_T(30) = 51.9$ ]. In nonpolar solvents ( $\text{CH}_2\text{Cl}_2$ ,  $E_T(30) = 40.9$ ), both nanoribbons and nanowires were obtained.

Figure 2 shows FT-IR spectra of peptide nanostructures obtained from various solvents. The IR spectra may provide information about intermolecular hydrogen bonding. As shown in Figure 2(a), spectra for the nanostructures formed in water and methanol have similar patterns, while the spectra formed in  $\text{CH}_2\text{Cl}_2$  is largely different. Nanoribbons formed in ethanol have an intermediate pattern between water and  $\text{CH}_2\text{Cl}_2$ . In  $\text{CH}_2\text{Cl}_2$  and ethanol, free N—H stretching peak is detected at  $3317 \text{ cm}^{-1}$  and a hydrogen bonded N—H stretching peak

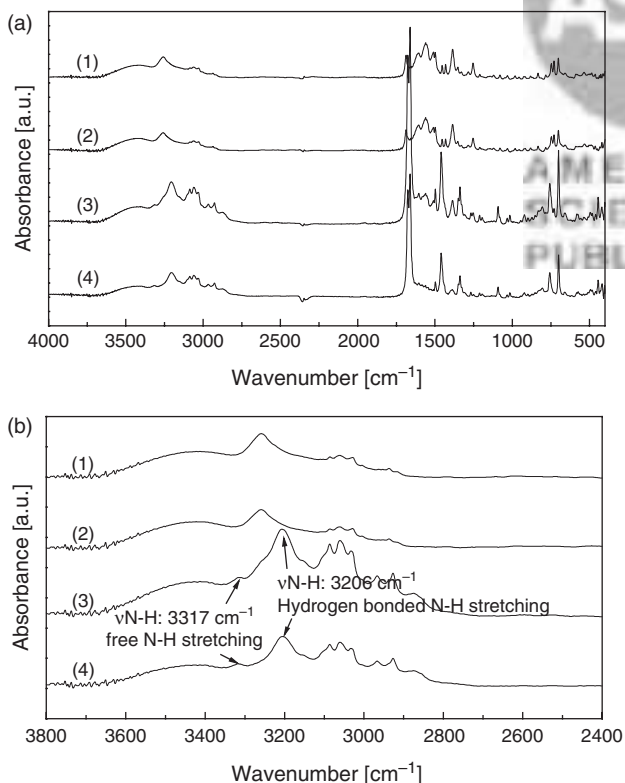


**Fig. 2.** (a), (b) FT-IR spectra of peptide nanostructures obtained in water (1), methanol (2), ethanol (3), and  $\text{CH}_2\text{Cl}_2$  (4) in a solid state.

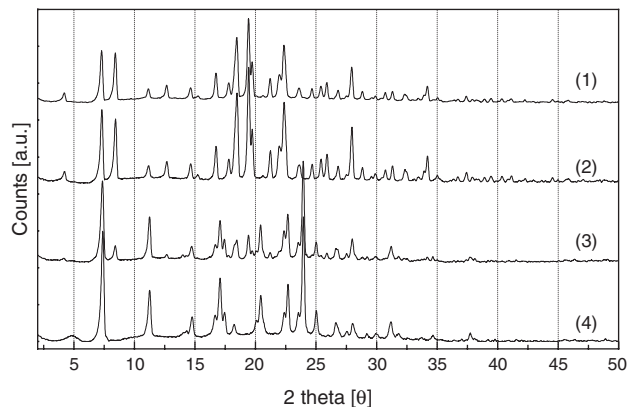


**Fig. 3.** XRD patterns of peptide nanostructures obtained in water (1), methanol (2), ethanol (3), and  $\text{CH}_2\text{Cl}_2$  (4).

is strongly represented at  $3206 \text{ cm}^{-1}$ .<sup>27</sup> From those spectra, the hydrogen bonding between dipeptide molecules is found to be a main interaction for assembly in ethanol and  $\text{CH}_2\text{Cl}_2$ . Also, a strong peak of  $3258 \text{ cm}^{-1}$  in a highly polar solvent (water and methanol) and a shoulder at the same position in ethanol are considered to occur due to the primary amine salt shifting to a higher frequency due to hydrophobic interaction. Thus, hydrophobic interaction is another key effect on the assembly in highly polar solvent. Note that hydrophobic attraction is a major interaction for assembly in water.<sup>28, 29</sup> In nonaqueous liquids, the attractive force is mainly dipolar interactions and specific intermolecular hydrogen bonding. Therefore, formation of nanotubes and nanoribbons is considered to originate from the subtle balance between hydrogen bonding and hydrophobic interaction.

Figure 3 shows powder X-ray diffraction patterns of diverse peptide nanostructures formed in different polar solvents. XRD patterns of nanotubes and nanoribbons, formed in water and methanol, have pattern similar to FT-IR patterns. From our previous results, it was revealed that those patterns represent the hexagonal packing of aromatic dipeptide.<sup>21</sup> Nanoribbons formed in ethanol have similar six major peaks so that nanoribbons have similar lattice with water and methanol, however, nanostructures formed in  $\text{CH}_2\text{Cl}_2$  have a different pattern. As shown in Figure 3, the  $d$ -spacing of the nanostructure prepared in water, methanol and ethanol is 2.1 nm, while the  $d$ -spacing of the nanostructure in  $\text{CH}_2\text{Cl}_2$  is 1.9 nm. The  $d$ -spacing of the nanostructure was calculated according to Bragg's law ( $\lambda = 2d \sin \theta$ ). The crystal structure of diverse nanostructures is still being investigated. However, the present results strongly support the notion that the specific hydrogen bonding between aromatic dipeptides affects the crystal structure.

#### 4. CONCLUSION

We have presented the synthesis of a variety of one-dimensional nanostructures consisting of an aromatic



dipeptide. Diverse morphologies ranging from nanotubes to nanoribbons and nanowires, were accomplished by changing the solvent polarity. Nanotubes were fabricated in water [ $E_T(30) = 80.0$ ] and nanoribbons were prepared in methanol [ $E_T(30) = 55.4$ ] and ethanol [ $E_T(30) = 51.9$ ]. In nonpolar solvents ( $\text{CH}_2\text{Cl}_2$ ,  $E_T(30) = 40.9$ ), both nanoribbons and nanowires were obtained. The morphological evolution of one-dimensional structures is assumed to originate from the subtle balance between hydrogen bonding and hydrophobic interaction. In nonpolar solvents, specific hydrogen bonding among aromatic dipeptides was a major interaction for assembly. Most significantly, the present results provide a versatile route to understand natural self-assembly into complicated architectures.

**Acknowledgment:** We thank Dr. Q. D. Nghiem for helpful discussions. This work was supported by the Korea Research Foundation (KRF-2005-003-D00085), the second stage of the Brain Korea 21 Project, the Basic Research Program of the Korea Science and Engineering Foundation (R01-2005-000-10456-0), R0A-2008-000-20057-0), the 21st Century Frontier Research Program (Center for Nanoscale Mechatronics & Manufacturing, 08K1401-01010) of the Ministry of Education, Science and Technology, the Korean Ministry of Science and Technology, the Fundamental R&D Program for Core Technology of Materials funded by the Ministry of Commerce, Industry and Energy, Republic of Korea.

## References and Notes

1. M. Sarikaya, C. Tamerler, A. K. Y. Jen, K. Schulten, and F. Baneyx, *Nat. Mat.* 2, 577 (2003).
2. S. Zhang, *Nat. Biotechnol.* 21, 1171 (2003).
3. G. M. Whitesides, J. P. Mathias, and C. T. Seto, *Science* 254, 1312 (1991).
4. J. D. Hartgerink, E. Beniash, and S. I. Stupp, *Science* 294, 1684 (2001).
5. A. Aggeli, L. A. Nyrkova, R. Harding, L. Carrick, T. C. B. McLeish, A. N. Semenov, and N. Boden, *Proc. Natl. Acad. Sci. USA* 98, 11857 (2001).
6. W. D. Jang, D. L. Jiang, and T. Aida, *J. Am. Chem. Soc.* 122, 3232 (2000).
7. S. Vauthey, S. Santoso, H. Gong, N. Watson, and S. Zhang, *Proc. Natl. Acad. Sci. USA* 99, 5355 (2002).
8. H. Matsui and B. Gologan, *J. Phys. Chem. B* 104, 3383 (2000).
9. D. T. Bong, T. D. Clark, J. R. Granja, and M. R. Ghadiri, *Angew. Chem. Int. Ed.* 40, 988 (2001).
10. X. Gao and H. Matsui, *Adv. Mat.* 17, 2037 (2005).
11. A. Nagai, Y. Nagai, H. Qu, and S. Zhang, *J. Nanosci. Nanotechnol.* 7, 2246 (2007).
12. J. Sun, X. Chen, C. Deng, H. Yu, Z. Xie, and X. Jing, *Langmuir* 23, 8308 (2007).
13. M. Morikawa, M. Yoshihara, T. Endo, and N. Kimizuka, *Chem. Eur. J.* 11, 1574 (2005).
14. S. Ghosh, M. Reches, E. Gazit, and S. Verma, *Angew. Chem. Int. Ed.* 46, 2002 (2007).
15. J. Kisiday, M. Jin, B. Kurz, H. Hung, C. Semino, S. Zhang, and A. J. Grodzinsky, *Proc. Natl. Acad. Sci. USA* 99, 9996 (2002).
16. F. Gelain, A. Lomander, A. L. Vescovi, and S. Zhang, *J. Nanosci. Nanotechnol.* 7, 424 (2007).
17. M. Yemini, M. Reches, E. Gazit, and J. Rishpon, *Anal. Chem.* 77, 5155 (2005).
18. T. Scheibel, R. Parthasarathy, G. Sawicki, X. M. Lin, H. Jaeger, and S. L. Lindquist, *Proc. Natl. Acad. Sci. USA* 100, 4527 (2003).
19. N. Nuraje, I. A. Banerjee, R. J. MacCuspie, L. Yu, and H. Matsui, *J. Am. Chem. Soc.* 126, 8088 (2004).
20. M. Reches and E. Gazit, *Science* 300, 625 (2003).
21. T. H. Han, J. Kim, J. S. Park, C. B. Park, I. Hyotcherl, and S. O. Kim, *Adv. Mater.* 19, 3924 (2007).
22. C. Reichardt, *Chem. Rev.* 94, 2319 (1994).
23. C. Reichardt, *Solvents and Solvent Effects in Organic Chemistry*, 2nd edn., VCH Publisher, Weinheim (1988).
24. J. Catalan and C. Diaz, *Liebigs Ann.* 9, 1942 (1997).
25. J. Catalan, C. Diaz, V. Lopez, P. Perez, J. L. G. de Paz, and J. G. Rodriguez, *Liebigs Ann.* 11, 1785 (1996).
26. J. G. Lu, R. Kong, and T. C. Chan, *J. Chem. Phys.* 110, 3003 (1999).
27. W. Zheng, M. Angelopoulos, A. J. Epstein, and A. G. MacDiarmid, *Macromolecules* 30, 2953 (1997).
28. P. Terech and R. G. Weiss, *Chem. Rev.* 97, 3133 (1997).
29. J. D. Hartgerink, J. R. Granja, R. A. Miligan, and M. R. Ghadiri, *J. Am. Chem. Soc.* 118, 43 (1996).

Received: 10 January 2008. Accepted: 20 February 2008.